

# FABRICATION OF A NOVEL MEMS CAPACITIVE MICROPHONE USING LATERAL SLOTTED DIAPHRAGM

*B. A. Ganji\* and M. S. Nateri*

*Department of Electrical Engineering, Babol University of Technology, 484 Babol, Iran  
Email: [baganji@nit.ac.ir](mailto:baganji@nit.ac.ir)*

\*Corresponding Author

(Received: February 4, 2010 – Accepted in Revised Form: November 15, 2010)

**Abstract** In this paper, we have fabricated a new microphone with lateral slotted diaphragm positioned over the back plate electrode using 8 anchors. It consists of a  $3\mu\text{m}$  thick aluminum (Al) as a diaphragm, a  $0.5\mu\text{m}$  as a back plate electrode and  $1.3\mu\text{m}$  thick resist (AZ1500) as a sacrificial layer on 4 inches silicon wafer. The novelty of this method relies on diaphragm which includes some lateral slots to reduce the effect of residual stress and stiffness of diaphragm for increasing the microphone sensitivity and also air damping in the gap has been reduced laterally. By this way, it is not needed to make acoustic holes in back plate, thus the effective surface of diaphragm has been increased and it causes to increase the microphone capacitance. Compared with previous works, the chip size of this microphone is reduced, the complex and expensive fabrication process can be avoided and the sensitivity can be increased. The measured zero bias capacitance of microphone is  $17.5\text{ pF}$ , and its pull-in voltage is  $25\text{ V}$ . The capacitance of the microphone was measured as a function of the applied bias voltage using C-V analyzer. The capacitance increased with increasing bias voltage due to the decrease in the air gap thickness as the Al membrane is electrostatically pulled towards the back plate. The microphone has been tested with external amplifier and speaker, the external amplifier was able to detect the sound waves from microphone on speaker and oscilloscope. The maximum amplitude of output speech signal of amplifier is  $45\text{ mV}$ , and the maximum output of MEMS microphone is  $1.125\mu\text{V}$ .

**Keywords** MEMS, Microphone, Lateral slots, Diaphragm stiffness

**چکیده** در این مقاله، یک میکروفون جدید ساخته شده که دارای شیارهای جانبی است و دیافراگم بوسیله ی ۸ پایه بر روی الکتروود زیرین قرار گرفته است. این میکروفون شامل یک دیافراگم آلومینیومی با ضخامت  $3\mu\text{m}$ ، یک لایه با ضخامت  $0.5\mu\text{m}$  بعنوان الکتروود زیرین و یک لایه ی مقاومت ضخیم با ضخامت  $1.3\mu\text{m}$  بعنوان لایه ی قربانی می باشد، که بر روی یک ویفر  $4\text{ اینچی}$  از جنس سیلیکون ساخته شده است. نوآوری این روش مربوط به ساخت دیافراگم که شامل چند شیار جانبی برای کاهش اثرات استرس پسماندی و سختی دیافراگم به منظور افزایش حساسیت میکروفون و همچنین خروج هوای موجود بین دو الکتروود بصورت جانبی می باشد. با این روش نیاز به ایجاد حفره های صوتی برای خروج هوا از روی الکتروود نمی باشد، بنابراین سطح موثر دیافراگم افزایش یافته و این باعث افزایش مقدار خازن میکروفون می شود. در مقایسه با کارهای گذشته، اندازه تراشه مورد نیاز برای میکروفون کاهش می یابد، می توان از پیچیدگی و گرانی فرآیند ساخت جلوگیری کرد و حساسیت می تواند افزایش یابد. مقدار خازن میکروفون اندازه گیری شده در بایاس صفر برابر با  $17.5\text{ pf}$  و ولتاژ اتصال آن برابر  $25\text{ v}$  است. خازن این میکروفون بعنوان تابعی از ولتاژ بایاس با استفاده از تحلیل گر  $\text{C-V}$  اندازه گیری شده است. مقدار این خازن با افزایش ولتاژ بایاس افزایش می یابد، بسبب کاهش فاصله ی هوایی که در نتیجه ی کشش نیروی الکترواستاتیکی بین الکتروود های خازن می باشد. این میکروفون بوسیله ی تقویت کننده و بلندگوی خارجی تست شده است، این تقویت کننده توانایی آشکارسازی شکل موج صوت را از میکروفون روی بلندگو یا دستگاه نمایش دارد. بیشترین دامنه ی سیگنال خروجی تقویت کننده برابر  $45\text{ mV}$  است و بیشترین خروجی میکروفون ساخته شده با استفاده از دانش MEMS برابر  $1.125\mu\text{V}$  است.

## 1. INTRODUCTION

A microphone is a transducer that converts acoustic energy into electrical energy. Microphones are widely used in voice communication devices, hearing aids, surveillance

and military aims, ultrasonic and acoustic distinction under water, and noise and vibration control [1]. Micromachining technology has been used to design and fabricate various silicon microphones. Among them, the capacitive microphone is in the majority because of its high

achievable sensitivity, miniature size, batch fabrication, integration feasibility, and long stability performance [2-4]. A capacitive microphone consists of a variable gap capacitor. To operate such microphones they must be biased with a dc voltage to form a surface charge [5, 6].

Most surface and bulk micromachined capacitive microphones use fully clamped diaphragm with perforated back plate [7, 8]. Typically, a cavity is etched into a silicon substrate by slope (54.74°) etching profiles using KOH etching, in order to form a thin diaphragm or perforated back plate [9-13]. Forming of a cavity or back chamber from the backside of wafer by KOH etching is slow and boring in that several hundred microns of substrate may need to be etched to make the chamber. Moreover, KOH etching process is not more compatible with CMOS process. Additionally, since the back plate needs acoustic holes which have to be etched from the back side in the deep back volume cavity, a nonstandard photolithographic process had to be used which needs electrochemical deposition of the photoresist and an aluminum seed layer. Process for fabrication of them are typically long, cumbersome, expensive, and not compatible with high volume process. Furthermore, they are not small in size.

An important performance parameter is the mechanical sensitivity of the diaphragm. The mechanical sensitivity of the diaphragm is determined by the material properties (such as Young's modulus and the Poisson ratio), thickness, and the intrinsic stress in the diaphragm. Very thin diaphragms are very fragile. In microfabrication, it is difficult to control the intrinsic stress levels in materials. In a prior paper [14], the stress problem was addressed by using a sandwich structure for diaphragms, in which layers with compressive and tensile stress were combined. If the diaphragm is composed of more than one material, this may induce a stress gradient because of the mismatch of the thermal expansions in the different materials. Any intrinsic stress gradient in the diaphragm material will cause diaphragm to bend, leading to a change of the air gap in the device, and therefore the sensitivity and cut-off frequency.

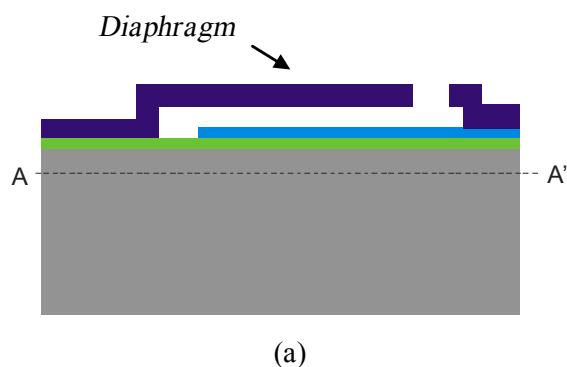
The objective in this paper is to overcome the disadvantages of the prior works by designing a novel MEMS capacitive microphone that utilizes a

lateral slotted diaphragm positioned over the back plate electrode using 8 anchors. The lateral slots reduces the air damping in the gap laterally, thus it is not needed to make acoustic holes in back plate and it also reduces the effect of residual stress and stiffness of diaphragm. By this way, the microphone size was reduced, and the sensitivity was increased.

## 2. MICROPHONE DESIGN

In this research a new MEMS capacitive microphone with lateral slotted diaphragm without acoustical holes positioned over the back plate electrode using 8 anchors has been designed and fabricated on 4 inches silicon wafer (see Figure 1). The novelty of this method relies on diaphragm which includes some lateral slots to reduce the effect of residual stress and stiffness of diaphragm and air damping in the gap. By this way, there is no need to make acoustic holes in back plate, thus the effective surface of diaphragm has been increased and it increases the microphone sensitivity. Compared with previous works, the chip size of this microphone is reduced, the complex and expensive fabrication process can be avoided, and the sensitivity can be increased.

In its simplest form, an acoustic wave striking the diaphragm causes its flexural vibration and changes the average distance from the back plate. The change of distance will produce a change in capacitance, giving rise to a time-varying voltage on the electrodes.



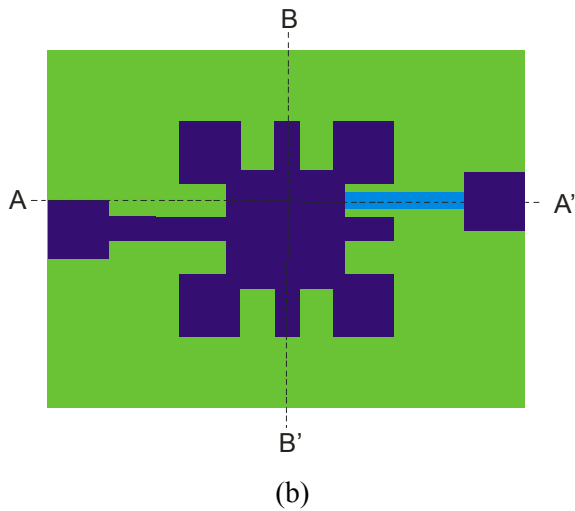


**Figure 1.** (a) Cross-section and (b) top view of lateral slotted microphone using 8 anchors

### 3. PROCESS FLOW

The whole process sequence uses three masks and several deposition, lithography and etching processes. The process starts with a single side polished silicon wafer as a substrate. The major fabrication steps are shown in Figure 2, and described as follow:

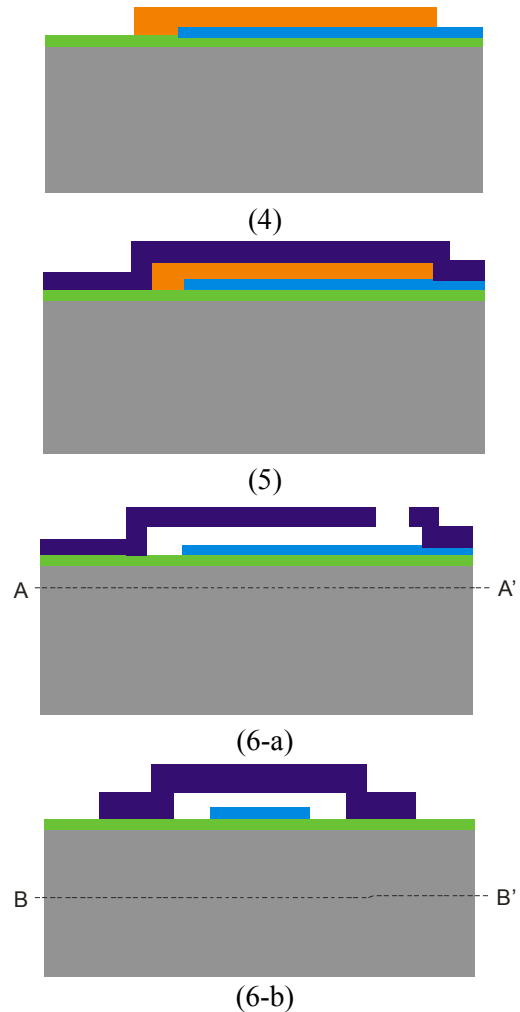
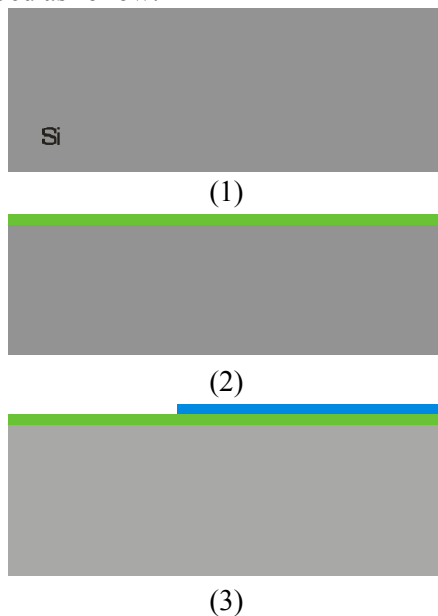


**Figure 2.** Fabrication process of the micro-machined capacitive microphone

1. First a 4-inch silicon wafer should be cleaned using standard cleaning procedure to remove organic contaminants such as dust particles, grease or silica gel and then any oxide layer should be removed from the wafer surface prior to processing. The first step in the cleaning process is to clean the wafer using ultrasonic method in the acetone solution for 5 minutes. The second step is to put the wafer in the methanol solution for 5 minutes. The final step is to dip the sample in a 10:1 DI water-HF solution (10% HF) until hydrophobicity is achieved (i.e. no water can stick to wafer). This will remove native oxide film.

2. A 2  $\mu\text{m}$  thick silicon oxide is sputtered on silicon wafer as an insulation layer.

3. A 0.3  $\mu\text{m}$  thick aluminum (Al) is sputtered and patterned as a back plate electrode. Al etch solution ( $\text{H}_3\text{PO}_4$ : 80 ml;  $\text{HNO}_3$ : 5 ml; DI water: 20

ml) was used to etch the sputtered Al.

4. A 1.3  $\mu\text{m}$  thick resist (AZ1500) was deposited and patterned in order to form a sacrificial layer.

5. A 2  $\mu\text{m}$  thick layer of aluminum is sputtered as a material of diaphragm. The Al layer is then patterned using positive resist mask to define the geometry of the diaphragm, contact pad, and anchors.

6. The sacrificial resist layer is etched using acetone to release the diaphragm. The fabrication process is completed by the release of the diaphragm by immersing it in deionized water (DI) and then acetone. Finally, the whole structure is dried on hot plate at 60  $^{\circ}\text{C}$  for 90 seconds to protect the diaphragm from sticking to the back plate.

#### 4. FABRICATION RESULTS

The purpose of this section is to examine the results from the fabrication and its meaning to the project.

##### 4.1. Silicon oxide isolating layer and aluminum back plate electrode

In our laboratory, first we have sputtered 2  $\mu\text{m}$  thick silicon oxide on silicon wafer as an insulation layer, then 0.5  $\mu\text{m}$  Al has been sputtered on silicon oxide as a back plate electrode. It was then patterned using photoresist mask and etched by Al etchant for 5 minutes. The etching rate of sputtered Al in Al etchant is 60 nm/minute.

##### 4.2. Resist (AZ1500) as a sacrificial layer

Deposition of sacrificial layer is an important step in MEMS device fabrication. Resist (AZ1500) is used as a sacrificial material. It can be easily deposited and removed using acetone. Moreover, acetone has a high selectivity to resist compared to silicon oxide and Al, thus it completely removes sacrificial resist without incurring significant damaging silicon oxide and Al. Sacrificial resist is usually deposited by spin coater. The deposition method chosen must be able to planarly deposit sacrificial layer on the structure. Spin coating is an alternative method to deposit planarized resist. The samples are spun for 30 seconds at 8000 rpm with 5 seconds pre-spin at 500 rpm to obtain 1.3  $\mu\text{m}$  thick sacrificial layer.

Baking is the most important process; the main purpose of baking is to remove solvent from resist. A few minutes of hot plate baking temperature of at least 100  $^{\circ}\text{C}$  is required to evaporate the solvent. The samples are then heated at 145  $^{\circ}\text{C}$  for 3 minutes. Figure 3 shows the optical microscopy top view of Al back plate electrode and photoresist (AZ1500) sacrificial layer on silicon oxide.

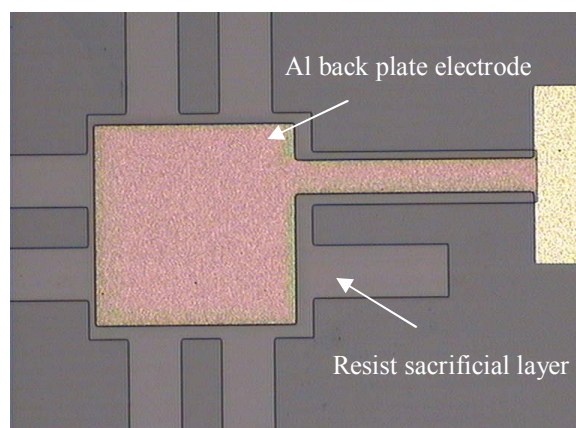


**Figure 3.** Optical microscopy top view of Al back plate electrode (0.5  $\mu\text{m}$ ) and photoresist (AZ1500) sacrificial layer (1.3  $\mu\text{m}$ ) on silicon oxide (2  $\mu\text{m}$ )

**4.3. Diaphragm making** A 3  $\mu\text{m}$  thick aluminum was deposited on resist sacrificial layer by DC sputtering, and patterned as a diaphragm.

**4.3.1. Al patterning** For patterning, first the positive photoresist (AZ1500) was spun on the structure. The starting cycle was set to 5 seconds, at a speed of 500 rpm. The second cycle was set for 30 seconds, with speed value of 2000 rpm. Once the spinning was completed, the wafer was baked in an oven for 2 minutes at 90 $^{\circ}\text{C}$ . After that, the wafer was brought to the mask aligner for exposure. The exposure was taken place for 60 seconds. This step was then followed by the agitated immersion of the wafer in photoresist developer (AZ300 MIF) to show the image. After that, the wafer has been rinsed in DI water to stop the development process.

**4.3.2. Al etching** Etchant for aluminum is 16:4:1 of phosphoric acid ( $\text{H}_3\text{PO}_4$ ), DI water, and nitric acid ( $\text{HNO}_3$ ). The etch rate of sputtered Al in Al etchant is 60 nm/min. First the structure was immersed in Al etchant for 35 minutes to etch the

Al for making diaphragm structure. A microscope was used to determine whether the Al had been removed and how successfully the Al was etched.

#### 4.4. Sacrificial resist etching using acetone

The approximate etch rate of Al in acetone in room temperature is zero. Therefore acetone shows a high selectivity against Al. For sacrificial layer etching, the structure was immersed in acetone bath to remove the sacrificial layer of resist. The wafers were placed directly onto the bottom of the bath's container and there was some agitation throughout the etching process. The wafers were taken out, and rinsed. Then the wafer was dried using hot plate at 60 °C for 90 seconds.

After completion of all processing on the wafers, the last step was to determine if the fabrication process had been successful. It is important to observe the silicon membrane and check to ensure that the resist layer was removed. All testing was performed by using a Scanning Electron Microscope (SEM) and optical microscope to capture images of the membrane surface and images of the cross-section. Figure 4 shows the top view of the fabricated microphone with Al diaphragm length of 0.5 mm.

Figure 5 shows the sacrificial layer etching for a microphone with diaphragm thickness of 3 μm, and air gap of 1.3 μm. It can be seen that, sacrificial layer has been removed under Al membrane completely, and Al membrane has been released.

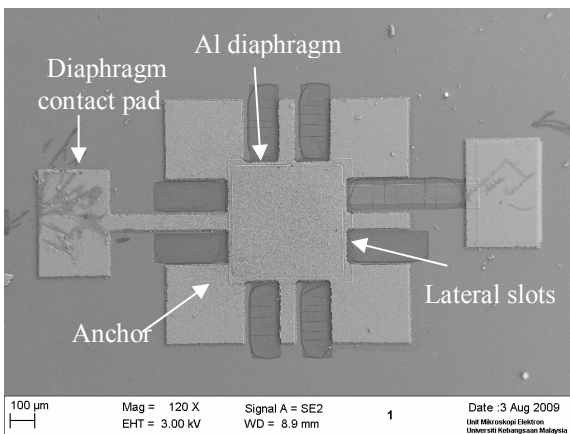


**Figure 4.** SEM image of top view of fabricated microphone

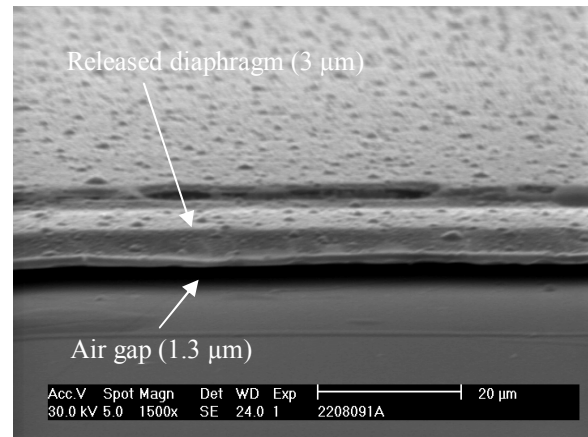


**Figure 5.** SEM images of released membrane of microphone

## 5. MEASUREMENTS AND TESTING

In this section, the microphone was tested to measure zero bias capacitance, pull in voltage, capacitance versus applied voltage between diaphragm and back plate, and microphone performance.

**5.1. Zero bias capacitance** The testing was done using the probe station, optical microscope, and LCR meter. The test set-up used to measure the sensor response is presented below. Figure 6 shows the measurement set-up for the silicon microphone. It is consisted of the microphone under test (MUT), the wafer stage, probe station, optical microscope and LCR meter. The set-up was arranged so that the microphone could be tested on the wafer.

The microphone was probed by probe needles that were connected to the computer, and the diaphragm deflection was observed and recorded. Next, the capacitance was measured and the zero bias capacitance, corresponding to an air gap of about 1 μm was 17.5 pF.

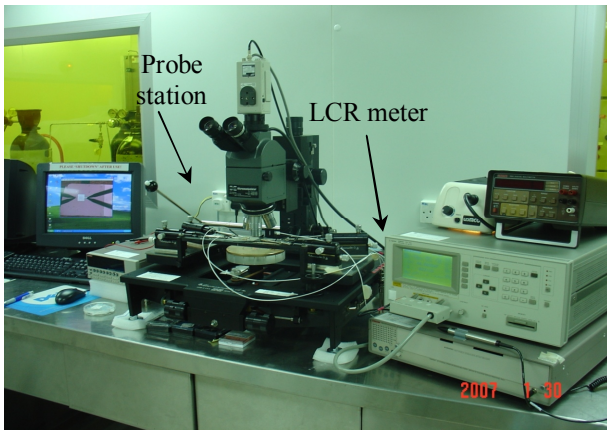


Figure 6. Complete measurement systems

**5.2. Pull-in voltage** Figure 7 shows the system set-up to measure the pull-in voltage of microphone. It is consisted of the microphone under test (MUT), the wafer stage, probe station, optical microscope, voltage source, and voltmeter. The microphone was probed by probe needles that were connected to the voltage source and voltmeter.

Figure 8 shows the structure and equivalent test circuit for  $V_{PI}$  measurement. The basic principle involves the well-known pull-in voltage. When a voltage  $V_b$  is applied across the air gap, the electrostatic force causes the diaphragm to deflect toward the substrate. An increase of the deflection of the membrane results in a decrease of the gap spacing and thus causes an increase of the electrostatic force.

If  $V_b$  exceeds the so-called pull-in voltage  $V_{PI}$ , the deflection does not reach an equilibrium position and will continue to increase until physical contact is made with the bottom electrode.

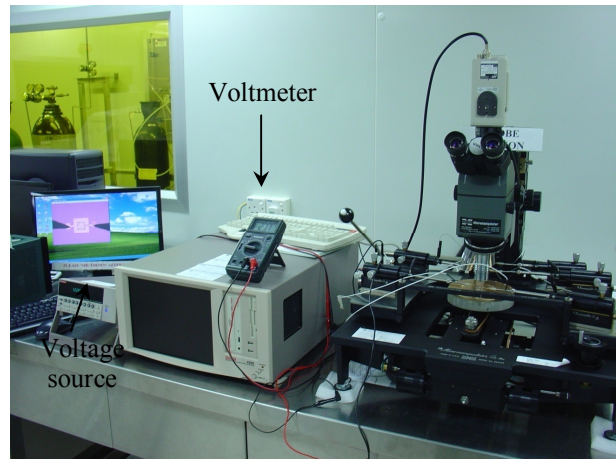
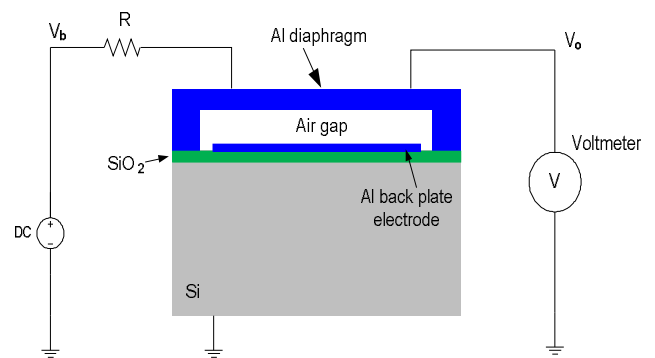
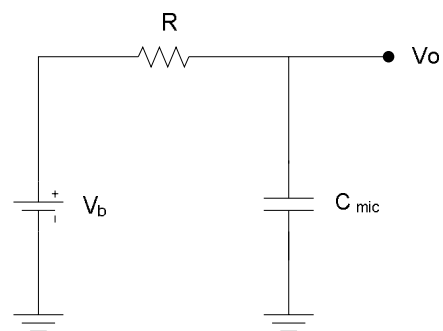


Figure 7. System setup to measure the pull-in voltage of microphone



(a)



(b)

Figure 8. Schematic diagrams of the (a) basic test structure and (b) equivalent circuit for VPI Measurement

$V_{PI}$  value was measured using the test circuit shown in Figure 8b.  $V_o$  maintains the same value

as  $V_b$ , ( $V_o = V_b$ ), and increases with  $V_b$  at the beginning. When  $V_b$  reaches  $V_{PL}$ ,  $V_o$  suddenly decreases, ( $V_o = 0$ ), because of the discharge of the conductive membrane (the upper electrode) due to the physical contact of the Al diaphragm and back plate electrode. As shown in Figure 9, the pull-in voltage of microphone is 25 V.

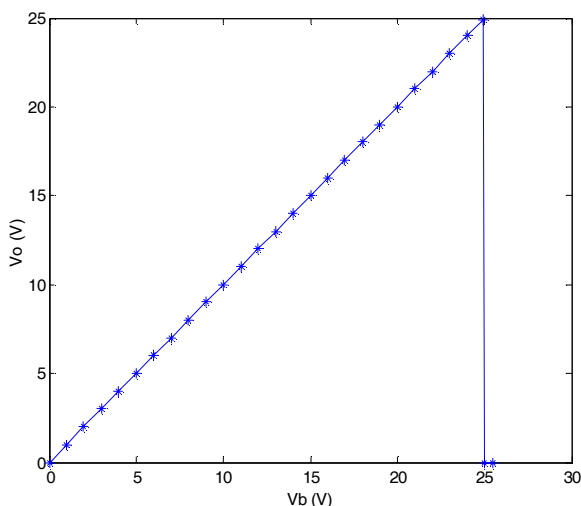


Figure 9. The variation of  $V_o$  with bias voltage,  $V_b$ ,

**5.3. Capacitance versus applied voltage** The capacitance of the microphone was measured as a function of the applied bias voltage using C-V analyzer. Figure 10 shows the measurement set-up for the microphone on the wafer. It is consisted of the microphone under test, the wafer stage, probe station, C-V analyzer, and chamber. The microphone was probed by probe needles that were connected to the C-V analyzer.

Figure 11 shows the capacitance versus bias voltage with a 0.5 mm diaphragm. The zero bias capacitance, corresponding to an air gap of about 1  $\mu\text{m}$  was 17.5 pF. The capacitance increased with increasing bias voltage due to the decrease in the air gap thickness as the Al membrane is electrostatically pulled towards the back plate. The bias voltage was increased from zero until 20V. From Figure 11, it can be seen that by increasing the voltage, the increasing of capacitance is not smooth, because the chamber is not insulated from acoustic waves.

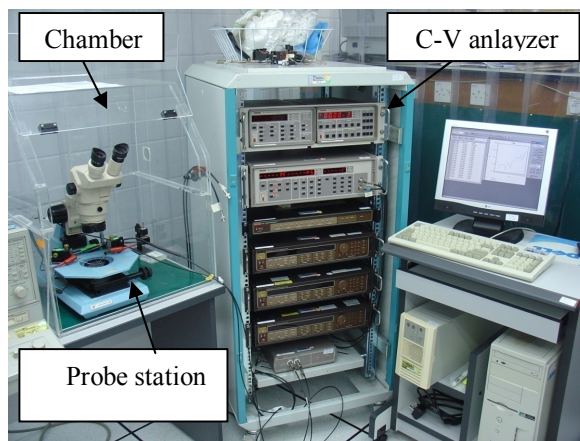


Figure 10. Measurement set-up to test of microphone on the wafer

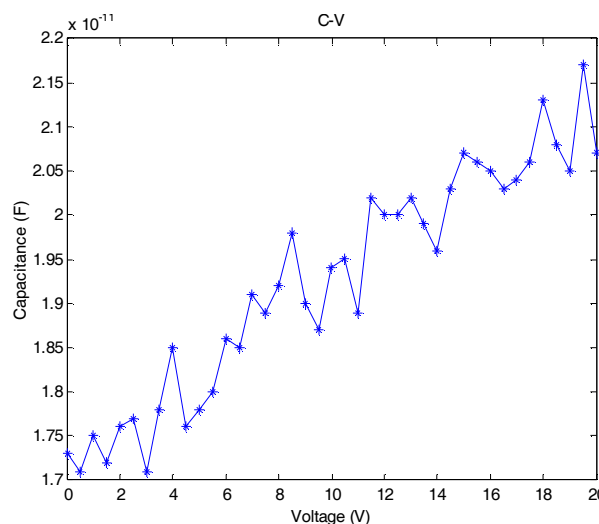
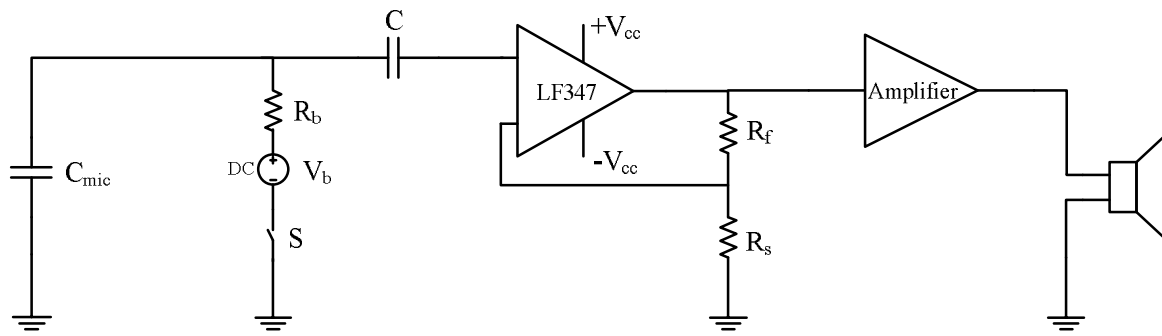


Figure 11. Capacitance of microphone versus voltage

#### 5.4. Test of microphone using external amplifier

Figure 12 shows the MEMS capacitive microphone connected to amplifier, power amplifier and speaker. The bias voltage of microphone is  $V_b = 3$  V, and bias resistance is  $R_b = 100$  M $\Omega$ . The amplifier consists of an operational amplifier LF347 with high input impedance of  $10^{12}$   $\Omega$ ,  $R_f = 1$  M $\Omega$ ,  $R_s = 1.25$  K $\Omega$ , and  $V_{cc} = 9$  V battery. The voltage gain of amplifier is  $A_{v1} = R_f/R_s = 800$ . The power amplifier is Radio shack- mini amplifier- speaker CAT. No. 277-1008°C.



**Figure 12.** Circuit diagram of external amplifier with speaker connected to MEMS microphone

The characteristics of power amplifier are as follow:

Input sensitivity: 1 mv

Input impedance: 5 K ohms

Power output (1 KHz): 200 mw (16 OHM load)

Distortion (1 KHz): <2%

Frequency response: 100Hz-10 KHz

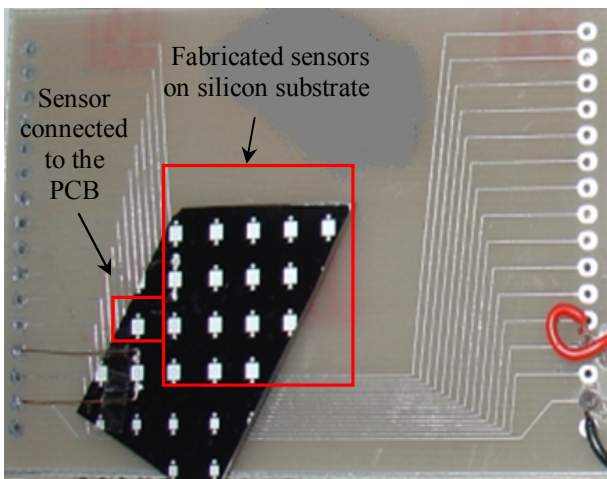
Power source of 9V battery or 9 VDC adapters

Speaker: DFE &A 220 16 Ω 0.5 W

The voltage gain of power amplifier is  $A_{v2} = 50$ .

The total voltage gain of external amplifier is  $A_{v_{tot}} = A_{v1} \cdot A_{v2} = 40000$ .

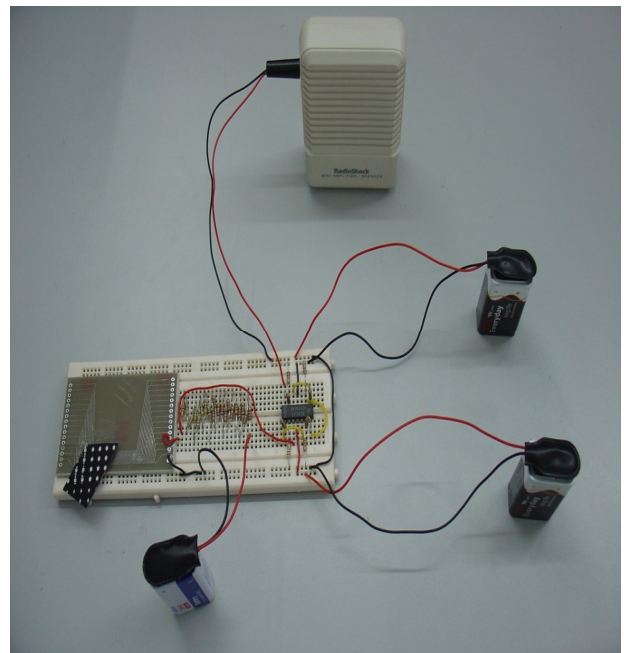
The fabricated microphone was manually wire bonded using copper wires and conductive silver paste on the sensor pads while the other end of the copper wires were soldered to the PCB signal lines. Figure 13 shows the fabricated sensor manually wire bonded to the sensor PCB.



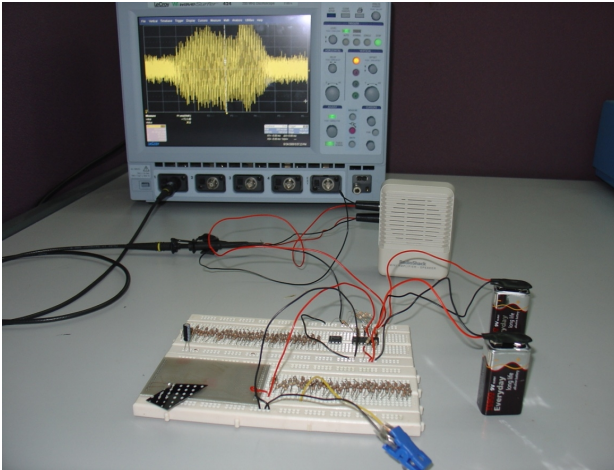
**Figure 13.** The fabricated sensor wire bonded to the sensor PCB

Figure 14 shows the practical circuit to test the microphone with human voice.

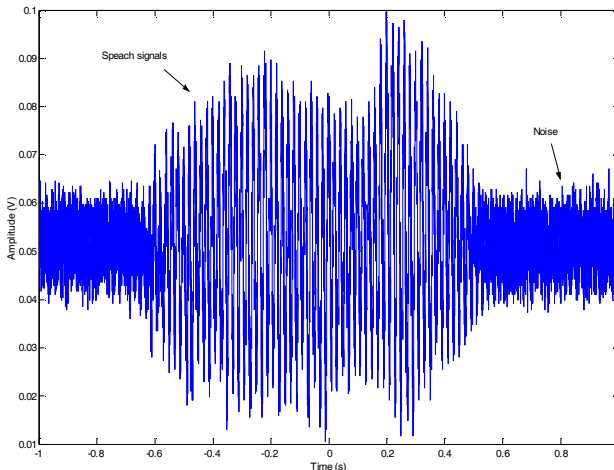
Figure 15a shows a complete system set-up prepared for the test of microphone with human voice. It can be seen that the external amplifier was able to detect the sound waves from microphone on oscilloscope. Figure 15b shows the 2 seconds of a speech signals applied to the microphone. From the Figure, the maximum amplitude of output speech signal of amplifier is 45 mV, thus the maximum output of MEMS microphone is 1.125 μV. The amplitude of the noise of amplifier is 10 mV.



**Figure 14.** A practical circuits to test themicrophone with human voice



(a)



(b)

**Figure 15.** (a) Complete system set-up (b) 2 seconds of a speech signals are applied to the microphone

## 6. CONCLUSION

In this paper, a new MEMS capacitive microphone has been designed and fabricated on 4 inches silicon wafer. The microphone consists of a lateral slotted diaphragm positioned over the back plate electrode using 8 anchors. The novelty of this method relies on the diaphragm includes some lateral slots to reduce the effect of residual stress and stiffness of diaphragm and also to reduce the air damping in the gap laterally. The advantages of this method are as follow: it is not needed to make acoustic holes and chamber in back plate, thus the

complex and expensive fabrication process can be avoided, the effective surface of diaphragm has been increased that it increases the microphone sensitivity and also the microphone size is reduced. By decreasing the diaphragm stiffness, the microphone sensitivity has been increased. The microphone has been fabricated and tested with Al diaphragm ( $t = 3 \mu\text{m}$ ,  $a = 0.5 \text{ mm}$ ,  $d = 1.3 \mu\text{m}$ ). The results of the fabrication process were noted through general observations and images gathered from optical microscope and SEM. The zero bias capacitance, corresponding to an air gap of  $1.3 \mu\text{m}$  was  $17.5 \text{ pF}$ , and the measured pull-in voltage was  $25 \text{ V}$ . The microphone has been tested with external amplifier and speaker, it can be seen that the external amplifier was able to detect the sound waves from microphone on speaker and oscilloscope. The maximum amplitude of output speech signal of amplifier is  $45 \text{ mV}$ , and the maximum output of MEMS microphone is  $1.125 \mu\text{V}$ .

## REFERENCES

1. T. Ma, T.Y. Man, Y. C. Chan, Y. Zohar, M. Wong, Design and fabrication of an integrated programmable floating-gate microphone. Proceedings of the Fifteenth IEEE International Conference on Micro Electro Mechanical Systems, (2002) pp. 288–291.
2. C. Jing, L. Liu, Z. Li, Z. Tan, Y. Xu, J. Ma, On the single-chip condenser miniature microphone using DRIE and back side etching techniques. Sens. Actuators, A 103 (2003) 42–47.
3. J. Miao, R. Lin, L. Chen, Q. Zou, S. Y. Lim, S. H. Seah, Design considerations in micromachined silicon microphones. Microelectronics Journal 33 (2002) 21-28.
4. X. Li, R. Lin, H. Kek, J. Miao, Q. Zou, Sensitivity-improved silicon condenser microphone with a novel single deeply corrugated diaphragm. Sensors and Actuators A 92 (2001) 257-262.
5. M. Pappalardo, G. Caliano, V. Foglietti, A. Caronti, E. Cianci, A new approach to ultrasound generation: the capacitive micromachined transducers. University Roma, Rome, Italy (2002).
6. M. Pappalardo, A. Caronti, A new alternative to piezoelectric transducer for NDE and medical applications: the capacitive ultrasonic micromachined transducer (cMUT). University Roma, Rome, Italy (2002).
7. J. Ning, Z. Liu, H. Liu, Y. Ge, A silicon capacitive microphone based on oxidized porous silicon sacrificial technology. Proc. 7<sup>th</sup> Int. Conf. on Solid-State and Integrated Circuits Technology, IEEE, 3 (2004) 1872–1875.
8. Y. B. Ning, A. W. Mitchell, R. N. Tait, Fabrication of a silicon micromachined capacitive microphone using a dry-etch process. Sens. Actuators, A 53 (1996) 237–242.

9. W. Kronast, B. Muller, W. Siedel, A. Stoffel, Single-chip condenser microphone using porous silicon as sacrificial layer for the air gap. *Sens. Actuators, A* 87 (2001) 188–193.
10. M. Pedersen, W. Olthuis, P. Bergveld, A silicon condenser microphone with polyimide diaphragm and back plate. *Sens. Actuators, A* 63 (1997) 97–104.
11. J. Bergqvist, J. Gobet, Capacitive microphone with a surface micromachined backplate using electroplating technology. *J. Microelectromech. Syst.* 3(2) (1994) 69–75.
12. A. Torkkeli, O. Rusanen, J. Saarilahti, H. Seppa, H. Sipola, J. Hietanen, Capacitive microphone with low-stress polysilicon membrane and high-stress polysilicon backplate. *Sens. Actuators* 85 (2000) 116–123.
13. A. E. Kabir, R. Bashir, J. Bernstein, J. De Santis, R. Mathews, J. O. O'Boyle, C. Bracken, Very High Sensitivity Acoustic Transducers with Thin P<sup>+</sup> Membrane and Gold Back Plate Sensors and Actuators-A, 78 (1999) 138-142.
14. P. Rombach, M. Mullenborn, U. Klein, K. Rasmussen, The first low voltage, low noise differential silicon microphone, technology development and measurement results. *Sens. Actuators, A* 95 (2002) 96–201.